Available online at www.sciencedirect.com
ScienceDirect
Journal of the European Ceramic Society 28 (2008) 837–842
www.elsevier.com/locate/jeurceramsoc

Screen printed low-sintering-temperature barium strontium titanate (BST) thick films

T. Tick *, J. Peräntie, H. Jantunen, A. Uusimäki

University of Oulu, Microelectronics and Materials Physics Laboratories and EMPART Research Group of Infotech Oulu, P.O. Box 4500, FIN 90014, Oulu, Finland

Received 19 June 2007; received in revised form 31 July 2007; accepted 19 August 2007
Available online 17 October 2007

Abstract

The dielectric properties of thick films based on Li_2O-doped $Ba_{0.55}Sr_{0.45}TiO_3$ powders were investigated. The powders were doped and prereacted at 500 °C, 700 °C and 900 °C for 10 h to lower their sintering temperature to a level of ~900 °C, enabling the use of silver electrodes. A fritless thick film paste was prepared by mixing ceramic powder with an organic medium, and thick films were screen printed on an Al_2O_3 (alumina) substrate together with silver electrodes. Printed parallel plate capacitor structures were used to characterize the dielectric properties. The films showed tunability of 30–34% at room temperature with a biasing field of 3 kV/mm. Their permittivity values were from 700 to 790 and their loss tangents were from 0.0042 to 0.0055 with a zero bias field at 10 kHz. The temperature dependence of permittivity was also measured, and the effect of porosity and grain size on the electrical performance of the films is discussed.

Keywords: BST; Thick film; Dielectric properties; Screen printing; (Ba, Sr)TiO_3

1. Introduction

Ferroelectric materials in the paraelectric state, especially barium strontium titanate (BST), have potential for use in tunable microwave applications such as resonators,[1] phase shifters,[2,3] filters[4] and antennas.[5,6] Previously, both screen printable and tape-cast-derived BST thick films have been studied because they reduce fabrication costs while offering moderate electrical properties compared with those of thin films.[7,8] Screen printing of thick films is a flexible, cost-effective fabrication method enabling relatively low film thickness, resulting in the use of lower biasing voltages compared with those of components prepared in bulk form. Preparation of screen printed BST thick films on Al_2O_3 (alumina) substrates has been studied and reported earlier.[9–11] However, the sintering temperatures of these films have been over 1200 °C, promoting the diffusion of barium into the alumina.[11] In addition, these high temperatures require the use of expensive refractory metals (e.g. platinum or palladium) instead of silver as the embedded and co-fired electrode material. Because of their low resistance, silver electrodes are preferred, especially in microwave applications. Also, lowering the sintering temperature of BST thick films below the melting point of silver (962 °C) allows their use with dielectric low-temperature co-fired ceramics (LTCC), thus enabling tunable components to be embedded in the future.

A lot of research has been done in order to lower the sintering temperature of BST powders below 900 °C by adding various sintering aids.[8,12,13] However, no reports have been published on the use of low-temperature sintering powders to prepare screen printed thick films compatible with silver electrodes. A method for lowering the sintering temperature of BST by prereaction and addition of Li_2O has been proposed by Valant and Suvorov.[13] The proposed method allows modification of the sintering rate by varying the prereaction temperature. This is an important advantage, since in preparing BST thick films, very rapid sintering kinetics are preferred in order to avoid diffusion between the BST, the electrode metal and the substrate material. Additionally, this helps to overcome constrictions in shrinkage inflicted by the rigid substrate.

The main objective of this study was to prepare fritless thick films using lithium-doped BST powders. The films were screen printed on alumina substrates and fired with silver

* Corresponding author. Tel.: +358 8 5532745; fax: +358 8 5532728.
E-mail address: ttick@ee.oulu.fi (T. Tick).

0955-2219/$ – see front matter © 2007 Elsevier Ltd. All rights reserved.
doi:10.1016/j.jeurceramsoc.2007.08.008

electrodes. The effect of different prereaction temperatures on the microstructures of the printed films and their electrical performance was studied. The microstructure of the films was also investigated and the dielectric properties and tunability of the films were measured. The effect of porosity and grain size on the electrical performance of the films is discussed.

2. Experimental

A commercial $0.99Ba_{0.55}Sr_{0.45}TiO_3 + 0.01TiO_2$ (BST–TIO) powder (Filtronic Comtek Ltd., Wolverhampton, UK) and Li_2CO_3 (Alfa Aesar GmbH & Co., Karlsruhe, Germany) as a sintering aid were used to fabricate the ceramic material for the paste. It was assumed that Li_2CO_3 decomposes to Li_2O and CO_2 during the prereaction. Thus, the desired doping level of 0.4 wt.% Li_2O was achieved by adding the corresponding molar fraction of Li_2CO_3. The materials were mixed in a planetary ball mill for 24 h with a ZrO_2 grinding media and acetone as a mixing vehicle. After drying, the powders were thermally treated to enable a prereaction of Li_2O with BST. This was done at three different temperatures of 500 °C, 700 °C and 900 °C, with a dwell time of 10 h. The corresponding powders and films are referred to as 500L04, 700L04 and 900L04. The powders were then hand ground and dry-milled for 1 h. The particle size distribution of the powders was measured with a laser diffraction particle size analyzer (LS230, Beckman Coulter Inc., California, USA).

The thick film pastes were prepared by adding 83 wt.% of BST powders to a commercial organic medium, N485 (Johnson Matthey Plc, London, UK), and mixing them in a triple roll mill for 30 min. The viscosity of the pastes was then measured at room temperature using a cone and plate rotation rheometer (Bohlin CS, Bohlin Reologi AB, Lund, Sweden). To characterize the dielectric properties of the films, thick film parallel plate capacitors were prepared by sequentially screen printing the bottom electrode, the BST film and the 5 mm × 5 mm top electrode. A 99.6% alumina substrate was used and the films were co-fired at 900 °C for 2 h. Silver paste (DuPont DP6160) was used for the electrodes. The thickness of the printed films was measured with a surface profiler (DekTak3ST, Veeco Instruments Inc., California, USA).

The crystalline phases of the compositions were studied using X-ray diffractometry (XRD; Philips, Germany). The microstructure of the films and the film interfaces were examined with scanning electron microscopy and energy dispersive spectroscopy (SEM, EDS; JSM-6400, JEOL, Tokyo, Japan). The density of the sintered films was estimated from the SEM images by calculating the ratio of the BST and void areas in the images and then transforming the area ratio to the corresponding volumetric ratio ($R_{\text{area}}^{3/2} = R_{\text{volume}}$). The area of the voids in the SEM image was differentiated from the area of the BST phase by their difference in tonal values. The relative permittivity and loss tangent of the films as a function of bias field and temperature were measured from the parallel plate capacitor samples with a precision LCR meter (4284A, Agilent Technologies Inc., California, USA) at 10 kHz, using an external voltage source (Agilent 6675A, Agilent Technologies Inc., California, USA) and a temperature chamber (SU-261, Espec Corp., Osaka, Japan).

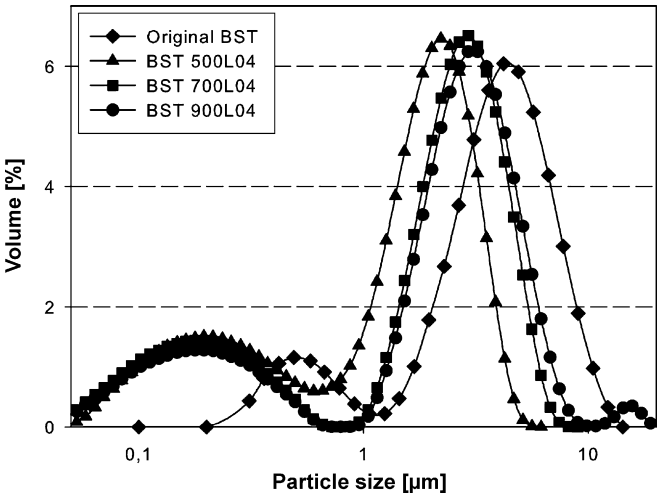

Fig. 1. Particle size distribution of the powders used in the paste preparation.

3. Results and discussion

The particle size distribution of the original BST–TIO was bimodal, which is typical for powders prepared with the conventional mixed oxide method (Fig. 1). The d_{50} value was 4.23 μm (Table 1). The ball milling performed before the prereaction reduced the average particle sizes, while the bimodal form of the particle size distribution remained relatively unchanged. The prereaction of BST–TIO with Li_2O increased the average particle size. The d_{50} value increased gradually from 1.75 μm to 2.67 μm because of sintering that occurred when the prereaction temperature was increased from 500 °C to 900 °C.

The viscosity measurements showed that the pastes had a shear thinning behaviour (Fig. 2). The discovered small hysteresis indicates thixotropic behaviour. The pastes prepared from 500L04, 700L04 and 900L04 powders had viscosities of 270 Pa s, 230 Pa s and 195 Pa s, respectively, at a shear rate of 10 s^{-1}. The prepared BST pastes had somewhat higher viscosity values than did commercial dielectric pastes. However, the printing characteristics of the BST pastes were adequate, since there was no need for accurate patterning of the films. The rheological behaviour of the pastes showed that the decrease in particle size increased the viscosity of the paste.

A film thickness of 30 μm was achieved with a single print using 325 mesh screens with a 16 μm emulsion. To avoid short circuiting pinholes in the capacitor samples, the printing was per-

Table 1
Mean particle sizes of the solids used in the paste preparation

Solid	d_{10} (μm)	d_{50} (μm)	d_{90} (μm)
BST–TIO	0.78	4.23	7.89
BST-500L04	0.17	1.75	3.29
BST-700L04	0.15	2.41	4.56
BST-900L04	0.16	2.67	5.27

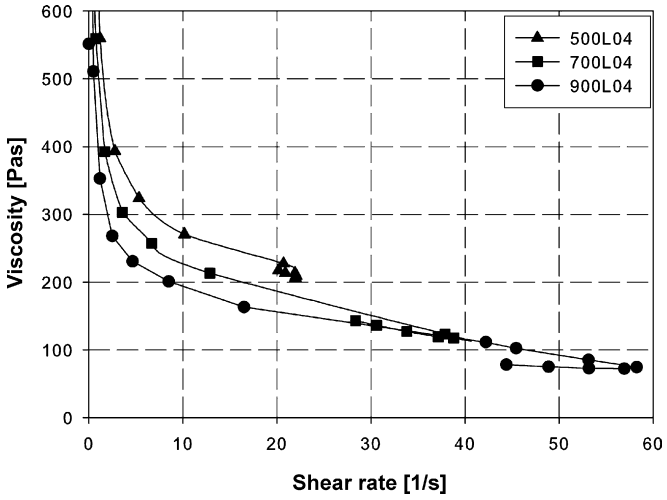

Fig. 2. Measured viscosities of the BST-based pastes as a function of shear rate.

formed twice. The sintered thickness of the films in the measured samples varied between 56 μm and 63 μm.

The phase structure of the films was investigated from films prepared on alumina substrates. The X-ray diffraction patterns of the films (Fig. 3) show that all the prepared films were clearly composed of a BST phase without detectable secondary phases. Peaks from the alumina substrate were also visible in the diffraction patterns.

All the fired films showed a somewhat porous microstructure (Fig. 4). The estimated density values were 72 vol.%, 68 vol.% and 68 vol.% for the 500L04, 700L04 and 900L04 films, respectively. Although the densities evaluated from the SEM images cannot be considered as absolute values, they can be used to compare the film densities. The microstructures and the estimated density values show that, in the sintering conditions we used, the powders with the lowest prereaction temperature and fastest sintering rate yielded films with the highest density. Additionally, the smaller particle size in the powders that were prereacted at lower temperatures may also enhance the density of the films, because of its larger specific surface area, which promotes sintering at lower temperatures. However, more research is needed in order to separate the effects of variation in the specific surface area of the powders from the effects of different prereaction temperatures on the density of the films.

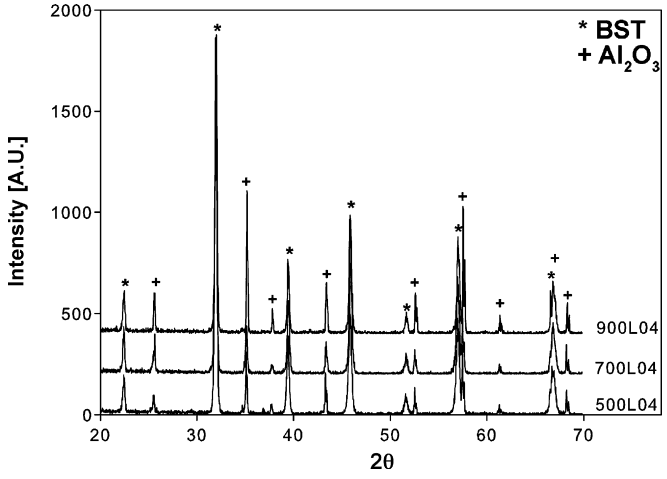

Fig. 3. X-ray diffraction patterns of the sintered Li_2O-doped $Ba_{0.55}Sr_{0.45}TiO_3$ thick films.

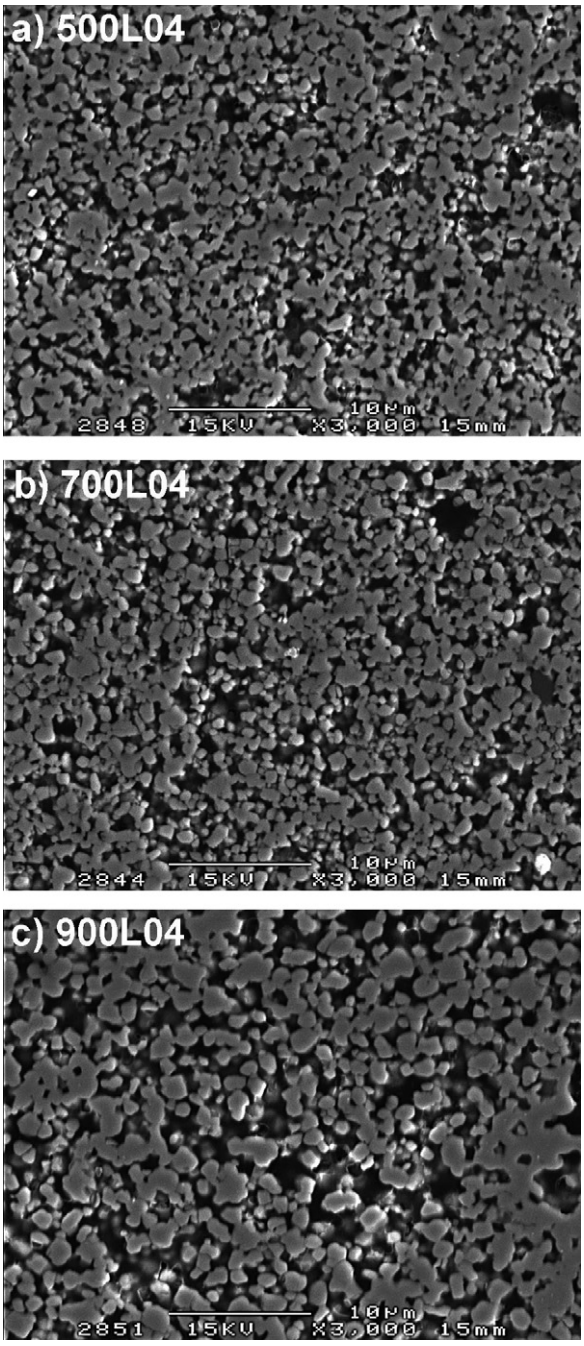

Fig. 4. (a–c) SEM images of sintered Li_2O-doped $Ba_{0.55}Sr_{0.45}TiO_3$ thick films.

The diffusion of different elements at the film interfaces was studied with EDS line analysis. Fig. 5a shows the interfaces between the BST film, the bottom silver electrode and the alumina substrate. A line scan of 20 μm was done over the BST–silver and silver–alumina interfaces, and the intensities of barium, strontium, aluminium and silver are presented in Fig. 5b. No significant diffusion between the materials was observed.

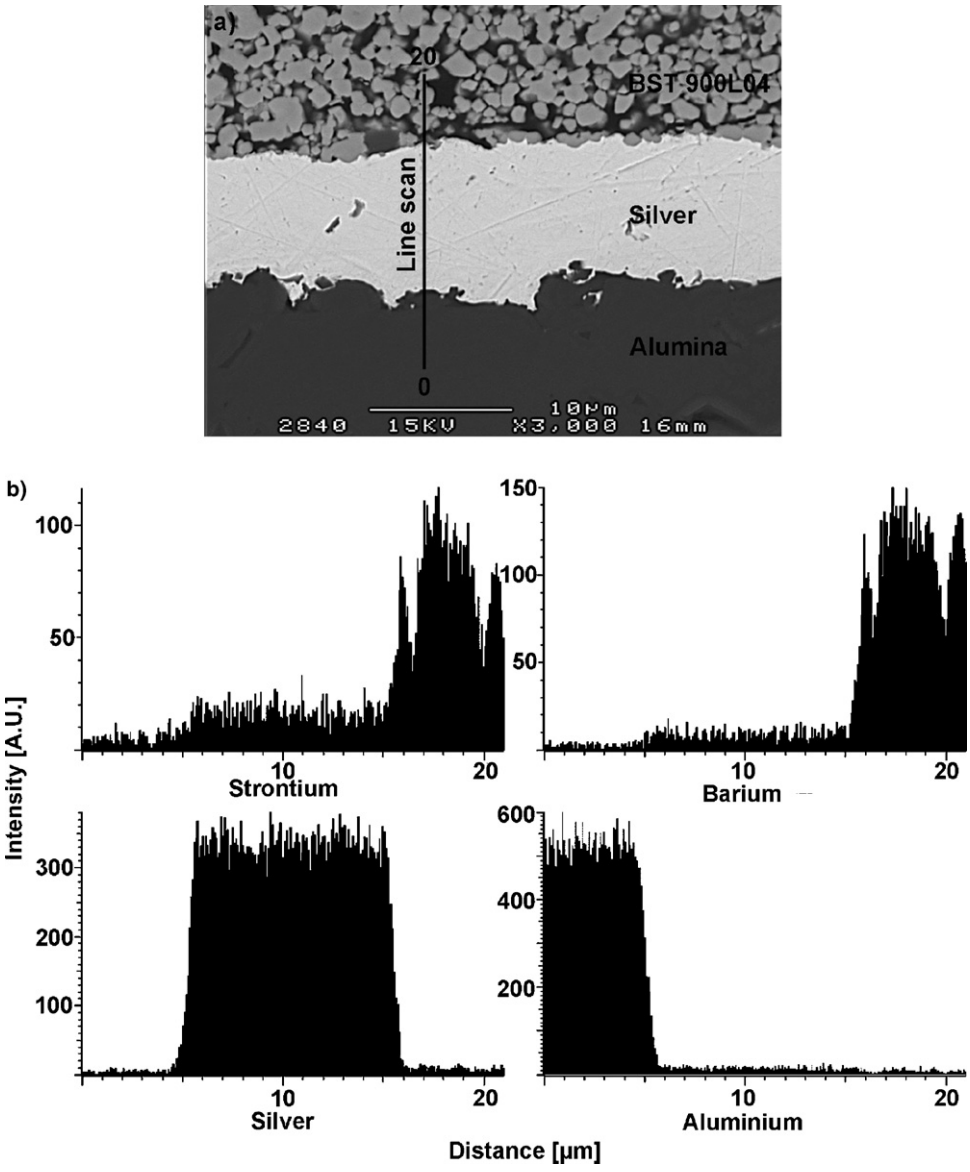

Fig. 5. (a) SEM-BSE image of the interfaces between the BST film, the bottom silver electrode and the alumina substrate. The black line indicates the position of the EDS line scan. (b) Amount of barium, strontium, aluminium and silver along the EDS line scan.

The measured relative permittivity (ε_r) as a function of temperature at 100 kHz shows that the ferroelectric to paraelectric (T–C) transition is very diffuse for all the samples (Fig. 6). It has been suggested that the compositional fluctuation of BST, i.e. the fluctuation of the Ba–Sr ratio in a sample, which creates phases with different T_c, broadens the T–C phase transition.[14] Although a notable shift of the XRD peaks of the measured films was not observed, possible fluctuation of the Ba–Sr ratio cannot be excluded. Similar broadening of the phase transition temperature may also be due to variance in lattice distortion. According to Liou et al., variation in the lattice distortion of the BST material depends on the grain size,[15] and since the T_c in the BST system is proportional to the lattice constant,[16] it affects the diffuseness of the T–C phase transition. As the grain size decreases, the T–C transition becomes more diffuse and both relative permittivity at T_c and tunability decrease.[15]

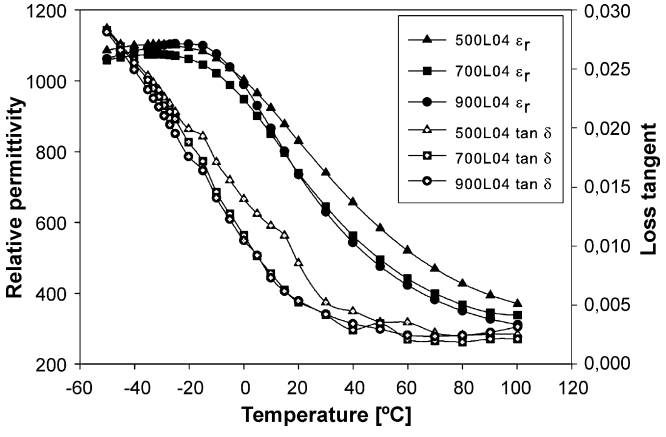

Fig. 6. Relative permittivity and loss tangent of the films as a function of temperature, measured at 10 kHz.

A trend of broadening of the T–C phase transition with the decreasing particle size of the initial powders can be noticed in the relative permittivity measurements (Fig. 6). The 500L04 film with the smallest initial particle size had the most diffuse T–C transition, whereas the 900L04 film with the largest initial particle size had the least diffuse transition, despite its lower density. As the density of the film decreases, the relative permittivity at T_c also decreases, and therefore the T–C phase transition of the material appears more diffuse in the relative permittivity measurements. The XRD patterns of the films did not show any signs of notable peak broadening, and thus no significant compositional fluctuation in the BST phase is expected. A possible explanation for the measured T–C transition narrowing could be grain growth during prereaction of the powders. Larger grain size results less diffuse T–C transition as stated before.

The loss tangent decreases linearly with increasing temperature near the T–C transition, indicating Curie–Weiss law behaviour. The 500L04 and 700L04 films go through the T–C transition at about a 6 °C lower temperature than the 900L04 film. This kind of decrease in the Curie temperatures with a decrease in grain size and porosity has been reported previously.[17,18]

The relative permittivities as a function of the bias field (E) are presented in Fig. 7. The relative permittivities of the 500L04, 700L04 and 900L04 films with a zero bias field were 790, 730 and 700, respectively, thus showing dependence on the density of the films. Tunability $n = (\varepsilon_r(T,0) - \varepsilon_r(T,E))/\varepsilon_r(T,0)$ under a bias field of 3 kV/mm was 32%, 34% and 30% for the 500L04, 700L04 and 900L04 films, respectively. The tunabilities of the films were quite similar, despite the differences in the particle size of the initial powders, film density and permittivity at zero bias. The measured tunability values were high compared with the value of 13.5 measured by Valant and Suvorov for Li_2O-doped $Ba_{0.60}Sr_{0.40}TiO_3$ bulk ceramics.[13] More studies are needed in order to fully understand the factors affecting the tunability of porous films and to explain the difference in tunability compared with bulk ceramics.

Measurement of dielectric loss as a function of the bias field showed behaviour similar to that of relative permittivity (Fig. 7). The losses were also found to be in a good agreement with the

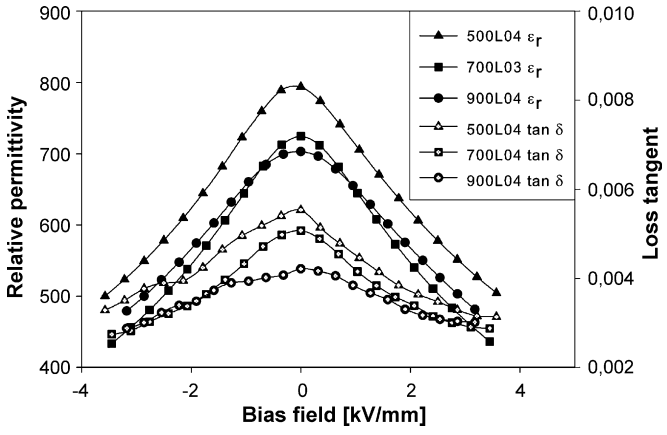

Fig. 7. Relative permittivity and loss tangent of the films as a function of bias field, measured at 10 kHz.

density of the films: the more porous the films, the lower the dielectric losses. The loss tangents of the films with a zero bias field were measured to be 0.0042, 0.0051 and 0.0055 for the 500L04, 700L04 and 900L04 films, respectively. It is assumed that the dielectric losses of BST films in the paraelectric state consist of intrinsic ($\tan\delta_C$) and conduction ($\tan\delta_R$) loss mechanisms. Johnson[19] has provided equations to describe the field dependence of both the imaginary and real parts of permittivity. A combination of these equations gives the intrinsic dielectric loss ($\tan\delta_C$) of the material:

$$\tan\delta_C = \frac{\tan\delta_{C_0}}{[1 + a\varepsilon'(T,0)^3 E^2]^{1/3}}, \quad (1)$$

where a is the phenomenological coefficient, $\tan\delta_{C_0}$ the intrinsic loss without an external bias field, $\varepsilon'(T,0)$ the real part of the relative permittivity with a zero field and T is the absolute temperature. On the other hand, conduction loss arises from the fact that a film possesses a finite resistance, which can be modelled as a parallel resistance with the tunable capacitor. In the case of a dc field this resistance is proportional to the biasing field through the nonlinear I–V characteristics, and the loss tangent of the conduction loss becomes:

$$\tan\delta_R = \frac{1}{\omega R\varepsilon'(T,E)C_0}, \quad (2)$$

where R is the resistance of the material, ω the measurement frequency and C_0 is the geometric capacitance.

The total dielectric loss of a material is the sum of these two previous mechanisms, which have opposing behaviours as a function of the dc field; with an increasing electric field the intrinsic loss decreases while the conduction loss increases. As we can see from Eqs. (1) and (2), both loss mechanisms are also temperature dependent through the variation of permittivity against temperature. When the temperature rises just above the Curie point, the permittivity is high and the intrinsic loss dominates over the negligible conduction loss component. Hence, the total loss decreases with an increasing bias field. At higher temperatures, the intrinsic loss decreases rapidly and the effect of the dc field E on the intrinsic losses is suppressed by the decrease of the product $a\varepsilon(T,0)^3$ in (1). Thus, the effect of the conduction loss on the total loss increases due to the decrease in permittivity, and total loss begins to increase with an increasing bias field. A specific temperature, called the "behaviour-transformation" temperature, T_b, can be found above which the conduction loss begins to dominate over the intrinsic loss and the dielectric loss starts to increase as a function of the biasing electric field.[15,20] The dc field behaviour of the measured dielectric losses implies the intrinsic-like dependence of the biasing field, where the loss tangent decreases rapidly with the increasing dc field. This behaviour shows that T_b of the BST material we used is higher than room temperature.

4. Conclusion

BST thick films were prepared by screen printing on alumina substrates. The sintering temperature of BST was lowered to 900 °C with lithium-based doping and by prereacting the pow-

ders. Lowering the sintering temperature allowed the use of silver electrodes. Different prereaction temperatures were used to study the effect of the prereaction temperature on the sintering kinetics and dielectric properties of the films. Thick films with a total thickness of approximately 60 μm were achieved by double printing. The films had permittivities ranging from 700 to 790 and loss tangents varying from 0.0042 to 0.0055 at 10 kHz. The highest measured tunability was 34% at 3 kV/mm. The dielectric loss was strongly affected by the porosity of the samples and the externally applied dc field. The larger the amount of air introduced into the ceramics, the smaller the measured dielectric loss. The field-induced decrease in dielectric loss indicates intrinsic loss behaviour, and thus the behaviour-transformation temperatures of all the printed films are above room temperature.

Acknowledgements

The author TT acknowledges the Foundation of Technology, the Seppo Säynäjäkangas Foundation and the Tauno Tönning Foundation for financial support of the work. The author JP acknowledges the Graduate School in Electronics, Telecommunications and Automation (GETA) for financial support of the work. The Finnish Funding Agency of Technology and Innovation (project number 52292) and its industrial partners are also acknowledged.

References

1. Ustinov, A. B., Tiberkevich, V. S., Srinivasan, G., Slavin, A. N., Semenov, A. A., Karmanenko, S. F. *et al.*, Electric field tunable ferrite–ferroelectric hybrid wave microwave resonators: experiment and theory. *J. Appl. Phys.*, 2006, **100**, 093905.
2. Zimmermann, F., Voigts, M., Weil, C., Jakoby, R., Wang, P., Menesklou, W. *et al.*, Investigation of barium strontium titanate thick films for tunable phase shifters. *J. Eur. Ceram. Soc.*, 2001, **21**, 2019–2023.
3. Yeo, K. S. K., Hu, W., Lancaster, M. J., Su, B. and Button, T. W., Thick film ferroelectric phase shifters using screen printing technology. In *Proceedings of the 34th European Microwave Conference*, 2004, pp. 1489–1492.
4. Scheele, P., Muller, S., Weil, C. and Jakoby, R., Phase-shifting coplanar stubline-filter on ferroelectric-thick film. In *Proceedings of the 34th European Microwave Conference*, 2004, pp. 1501–1504.
5. Varadan, V. K., Jose, K. A. and Varadan, V. V., Design and development of electronically tunable microstrip antennas. *Smart Mater. Struct.*, 1999, **8**, 238–242.
6. Castro-Vilaro, A. M. and Solis, R. A. R., Tunable folded-slot antenna with thin film ferroelectric material. In *Proceedings of the IEEE International Symposium of Antennas and Propagation*, 2003, pp. 549–552.
7. Su, B. and Button, T. W., The processing and properties of barium strontium titanate thick films for use in frequency agile microwave circuit applications. *J. Eur. Ceram. Soc.*, 2001, **21**, 2641–2645.
8. Hu, T., Jantunen, H., Uusimäki, A. and Leppävuori, S., $Ba_{0.7}Sr_{0.3}TiO_3$ powders with B_2O_3 additive prepared by the sol–gel method for use as microwave material. *Mater. Sci. Semicond. Process*, 2002, **5**, 215–221.
9. Zimmermann, F., Voigts, M., Menesklou, W. and Ivers-Tiffée, E., $Ba_{0.6}Sr_{0.4}TiO_3$ and $BaZr_{0.3}Ti_{0.7}O_3$ thick films as tunable microwave dielectrics. *J. Eur. Ceram. Soc.*, 2004, **24**, 1729–1733.
10. Su, B., Holmes, J. E., Meggs, C. and Button, T. W., Dielectric and microwave properties of barium strontium titanate (BST) thick films on alumina substrates. *J. Eur. Ceram. Soc.*, 2003, **23**, 2699–2703.
11. Ditum, C. M. and Button, T. W., Screen printed barium strontium titanate films for microwave applications. *J. Eur. Ceram. Soc.*, 2003, **23**, 2693–2697.
12. Rhim, S. M., Hong, S., Bak, H. and Kim, O. K., Effects of B_2O_3 addition on the dielectric and ferroelectric properties of $Ba_{0.7}Sr_{0.3}TiO_3$ ceramics. *J. Am. Ceram. Soc.*, 2000, **83**, 1145–1148.
13. Valant, M. and Suvorov, D., Low-temperature sintering of $(Ba_{0.6}Sr_{0.4})TiO_3$. *J. Am. Ceram. Soc.*, 2004, **87**, 1222–1226.
14. Diamond, H., Variation of permittivity with electric field in perovskite-like ferroelectrics. *J. Appl. Phys.*, 1961, **32**, 909–915.
15. Liou, J. and Chiou, B., DC field dependence of the dielectric characteristics of doped $Ba_{0.65}Sr_{0.35}TiO_3$ with various grain sizes in the paraelectric state. *Jpn. J. Appl. Phys.*, 1997, **36**, 4359–4368.
16. Lemanov, V. V., Smirnova, E. P., Syrnikov, P. P. and Tarakanov, E. A., Phase transitions and glasslike behavior in $Sr_{1-x}Ba_xTiO_3$. *Phys. Rev. B*, 1996, **54**, 3151–3157.
17. Zhang, L., Zhong, L., Wang, C. L., Zhang, P. L. and Wang, Y. G., Dielectric properties of $Ba_{0.7}Sr_{0.3}TiO_3$ ceramics with different grain size. *Phys. Stat. Sol. (A)*, 1998, **168**, 543–548.
18. Fang, T., Hsieh, H. and Shiau, F., Effects of pore morphology and grain size on the dielectric properties and tetragonal–cubic phase transition of high-purity barium titanate. *J. Am. Ceram. Soc.*, 1993, **76**, 1205–1211.
19. Johnson, K. M., Variation of dielectric constant with voltage in ferroelectrics and its application to parametric devices. *J. Appl. Phys.*, 1962, **33**, 2826–2831.
20. Liou, J. and Chiou, B., Effect of direct-current biasing on the dielectric properties of barium strontium titanate. *J. Am. Ceram. Soc.*, 1997, **80**, 3093–3099.